

Effect of pressure on the quantum spin ladder material IPA-CuCl₃

Tao Hong, V. O. Garlea, A. Zheludev, and J. A. Fernandez-Baca
Neutron Scattering Sciences Division, Oak Ridge National Laboratory, Oak Ridge, Tennessee 37831-6393, USA

H. Manaka
Graduate School of Science and Engineering, Kagoshima University, Korimoto, Kagoshima 890-0065, Japan

S. Chang, J. B. Leao, and S. J. Poulton*
NIST Center for Neutron Research, National Institute of Standards and Technology, Gaithersburg, Maryland 20899, USA
 (Received 8 September 2008; revised manuscript received 7 November 2008; published 10 December 2008)

Inelastic-neutron-scattering and bulk magnetic-susceptibility studies of the quantum $S=1/2$ spin ladder system $(\text{CH}_3)_2\text{CHNH}_3\text{CuCl}_3$ are performed under hydrostatic pressure. The pressure dependence of the spin gap Δ is determined. At $P=1500$ MPa it is reduced to $\Delta=0.79$ meV from $\Delta=1.17$ meV at ambient pressure. The results allow us to predict a soft-mode quantum phase transition in this system at $P_c \sim 4$ GPa. The measurements are complicated by the proximity of a structural phase transition that leads to a deterioration of the sample.

DOI: [10.1103/PhysRevB.78.224409](https://doi.org/10.1103/PhysRevB.78.224409)

PACS number(s): 75.10.Jm, 75.25.+z, 75.50.Ee

I. INTRODUCTION

Phase transitions in quantum spin liquids have recently been attracting a great deal of attention.¹ Such systems remain disordered at $T=0$ due to zero-point quantum spin fluctuations and have an energy gap Δ in the magnetic excitation spectrum. If changing some external parameter, such as magnetic field or hydrostatic pressure, reduces the gap energy, a soft-mode quantum phase transition can be expected at the point where $\Delta \rightarrow 0$. Beyond the phase transition the system typically develops long-range magnetic order in the ground state. Field-induced ordering transitions are the easiest to realize experimentally and the most extensively studied.²⁻⁶ In that scenario one of the three lowest-energy $S=1$ gap excitations is driven to zero energy by virtue of the Zeeman effect. In a Heisenberg spin-gap system such a transition breaks $\text{SO}(2)$ symmetry and is famously described as a Bose-Einstein condensation (BEC) of magnons.⁷

Less studied are transitions driven by external pressure. These may occur in materials in which pressure-induced lattice distortions modify the exchange constants or magnetic anisotropy in such a way as to reduce the gap energy.⁸ The transition is distinct from BEC in that it leads to a spontaneous violation of $\text{SO}(3)$ symmetry in a Heisenberg system. To date, only one experimental realization of this latter mechanism has been found, namely, in the $S=1/2$ spin-dimer system TiCuCl_3 . This compound was thoroughly studied by bulk measurement⁹ and neutron-scattering measurement.^{10,11} It is extremely sensitive to the effect of pressure and the transition is observed at a critical value as low as $P_c = 107$ MPa.

The present work focuses on another prototypical quantum spin liquid, namely, the $S=1/2$ quantum spin ladder material $(\text{CH}_3)_2\text{CHNH}_3\text{CuCl}_3$ (IPA-CuCl₃, where IPA denotes isopropyl ammonium).¹²⁻¹⁴ The crystal structure and topology of magnetic interactions in this Heisenberg antiferromagnet were discussed in detail in Ref. 12. Cu^{2+} -based $S=1/2$ ladders with antiferromagnetic (AF) leg coupling run along the **a** axis of the triclinic $P\bar{1}$ crystal structure. Spin

correlations along the ladder rungs are ferromagnetic. Additional nonfrustrating AF interactions are along the ladder diagonals. The ground state is a spin singlet with a spin gap $\Delta=1.17$ meV. Small but measurable interactions between ladders account for a weak dispersion of gap excitations along the crystallographic **c** axis. Interactions along the **b** axis are negligible, as is magnetic anisotropy. The global minimum of the three-dimensional (3D) dispersion is located at the magnetic zone center (0.5,0,0). It is at this point where a magnetic Bragg peak appears when BEC of magnons and long-range ordering are induced in IPA-CuCl₃ by an external field exceeding $H_c=9.7$ T.^{6,15} The main purpose of the present experiments is to attempt to suppress the gap and potentially induce an ordering transition in IPA-CuCl₃ by applying hydrostatic pressure, rather than a magnetic field.

II. BULK MEASUREMENTS

While less straightforward to interpret, bulk magnetic measurements are typically much easier to perform under pressure than neutron-scattering experiments. For IPA-CuCl₃ we investigated the temperature dependence of the magnetic susceptibility down to $T=1.8$ K, using a superconducting quantum-interference device (SQUID) magnetometer in a dc field of 1 T and single-crystal samples with a typical size of $2 \times 6 \times 1$ mm³. Pressures of up to 810 MPa were achieved using a TiCu piston cylinder clamp cell¹⁶ that was loaded at room temperature. The pressure medium was a mixture of two types of fluid Fluorinert (FC70:FC77=1:1). The produced pressure around 4.2 K was calibrated as a function of the applied load by means of the Meissner effect of Sn. Sample data are shown in Fig. 1. At ambient pressure (open circles) the susceptibility curve is consistent with that reported in Ref. 13. The broad rounded maximum at $T \approx 20$ K is characteristic of low-dimensional Heisenberg antiferromagnet. The behavior of quickly decreasing toward zero at low temperatures indicates that the ground state is the singlet state. This exponentially activated character is a sig-

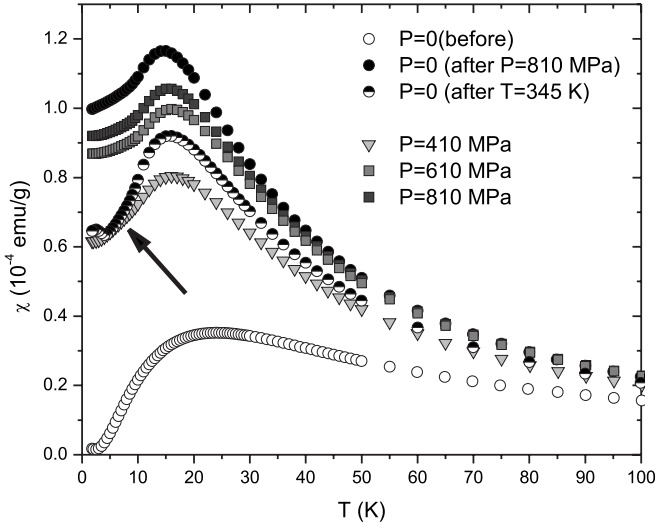


FIG. 1. Temperature dependence of the magnetic susceptibility in IPA-CuCl₃ is measured at various pressures in a dc field of 1 T. Samples previously pressurized to 810 MPa (solid circles) show a behavior different from that of never pressurized ones (open circles), but similar to that of those that have gone a structural transition at $T=323$ K at ambient pressure (half-filled circles). The error bars are smaller than the data points. The arrow indicates a nonactivated contribution at $T \rightarrow 0$.

nature of a spin gap. At an applied pressure of $P=410$ MPa the low-temperature behavior changes qualitatively. Rather than dropping to zero, the $\chi(T)$ tends to a finite value at the lower end of the measurement range. The trend continues up to 810 MPa, with the low-temperature value steadily increasing. An unusual observation is the irreversibility of this effect: releasing the external pressure *does not return the susceptibility to its original values* (open circles in Fig. 1). Pressurizing the samples also has an irreversible effect on their visual appearance. As-grown crystals are dark red or brown, while those previously pressurized to 810 MPa acquire a pale beige color.

The irreversibility is clearly caused by structural damage to the samples, which in turn is likely due to a pressure-induced crystallographic transition. Indeed, IPA-CuCl₃ is known to be close to a structural phase boundary. At ambient pressure it undergoes a structure phase transformation at $T=323$ K.¹⁷ This transition induces the same kind of color change in IPA-CuCl₃ single crystals as the application of pressure. The crystal structure at high-temperature phase consists of linear chains and three Cu-Cl-Cu superexchange paths.¹⁷ The $\chi(T)$ curves for crystals previously taken through the $T=323$ K transition (Fig. 1, half-filled circles) are also qualitatively similar to those collected in previously pressurized samples.

One can expect that the microscopic fracturing induced by the phase transition will have an effect on the spin ladders in IPA-CuCl₃ similar to what microfine grinding has on the Haldane spin chain material Ni(C₃H₁₀N₂)₂N₃(ClO₄) (NINAZ).¹⁸ A fragmentation of the ladders will release $S=1/2$ degrees of freedom on the ends of every finite-length fragment. These free spins will constitute the dominant contribution to susceptibility and specific heat at low tempera-

tures, where the contribution of uninterrupted ladder sections is exponentially small. Thus, any effect of the applied pressure on the spin gap is masked by the appearance of end-chain spins, and therefore cannot be conclusively investigated by bulk susceptibility or calorimetric techniques. In this case, furthermore, pressure dependence of $\chi(T)$ curves do not show a systematic behavior because the sign as well as the absolute value of the rung exchange interaction is sensitive not only to the Cu-Cl-Cu bonding angle but also to the dihedral folding angle and twisting angle of the Cu₂Cl₆ dimer planes.¹⁹

III. NEUTRON-SCATTERING MEASUREMENTS

The end-chain spins that interfere with bulk measurements have no intrinsic dynamics and therefore do not severely affect inelastic neutron experiments. The gap excitations in IPA-CuCl₃ were studied under pressure in two separate runs on the SPINS three-axis cold-neutron spectrometer at NIST. A pyrolytic graphite (PG) PG(002) monochromator was used in conjunction with a flat (setup 1) or horizontally focusing (setup 2) PG analyzer. The incident-beam divergence was controlled by the ⁵⁸Ni guide before the monochromator. For setup 1 an 80' Soller collimator was placed between the sample and analyzer, while a 120' radial collimator was used for setup 2. The final energy was fixed at $E_f=5$ meV (setup 1) or 3.7 meV (setup 2) and a Be (setup 1) or BeO (setup 2) low-pass filter was placed after the sample.

In the first series of measurements (setup 1), we utilized an aluminum He-gas cell that delivered pressure of up to 650 MPa. This cell has a neutron transmission of 65%, and the pressure can be changed *in situ*, without warming the sample up to room temperature, though the P - T curve for helium must be considered. Five fully deuterated single crystals with a total mass of ≈ 150 mg were coaligned to an irregular mosaic spread of 2° full width at half maximum (FWHM) at ambient pressure (each individual crystal had a mosaic of about 0.5° FWHM). Increasing the pressure to 620 MPa had no effect on sample mosaic.

The second setup (setup 2) utilized the Al₂O₃ clamp-type pressure cell as described in detail in Ref. 20. For this cell neutron transmission is strongly energy dependent and can be as low as 10%.²¹ Due to the cell design, it can only be loaded incrementally, each pressure change requiring its removal from the cryostat at room temperature. In the experiment we utilized a 300 mg deuterated single-crystal IPA-CuCl₃ sample with an initial mosaic spread of about 0.5° . The pressure medium was fluid Fluorinert FC-75. All data were collected at $P=1500$ MPa where the mosaic of the crystal was Gaussian in shape but irreversibly broadened to as much as 5.5° . The actual value of the applied pressure was determined by measuring the d spacing in a single crystal of NaCl loaded in the same cell, following Ref. 20. Attempting to pressurize the sample beyond 1500 MPa resulted in collapse of the sample. In both experiments the sample environment was a He-flow cryostat, enabling data collection at $T=1.5$ K.

All the data were taken in constant- \mathbf{q} scans at the magnetic zone center (0.5,0,0). The data obtained using setup 2

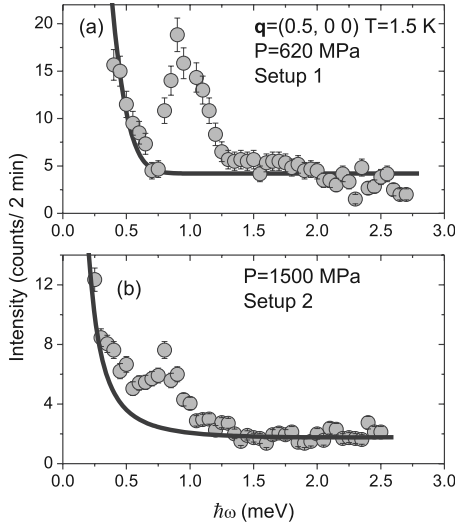


FIG. 2. Typical constant- \mathbf{q} scans (raw data) collected at the magnetic zone center in IPA-CuCl₃ at (a) $P=620$ MPa using setup 1 (symbols) and (b) $P=1500$ MPa using setup 2 (symbols). The solid lines are a model for the background contribution, as described in the text. Error bars represent one standard deviation determined assuming Poisson statistics.

were corrected for the energy dependence of neutron absorption using the results of Ref. 21. The following procedure was used to determine the background. In setup 1, beyond 0.8 meV energy transfer it was measured away from the magnetic zone center at wave vectors (0.3,0,0) and (0.75,0,0), and fits to a straight line. In the range of 0.2–0.8 meV it was taken directly from the (0.5,0,0) scan at ambient pressure, where no magnetic scattering is expected due to a 1.2 meV spin gap, and fits to an additional Gaussian profile to account for elastic incoherent scattering in the sample environment and thermal diffuse scattering in the monochromator. In setup 2, constant- \mathbf{q} scans of (0.3,0,0) and (0.75,0,0) were also measured and the background was taken into account as a fit to a Gaussian profile. Figure 2 shows raw data measured using: (a) setup 1 at 620 MPa (symbols) and (b) setup 2 at 1500 MPa (symbols) along with the estimated background contribution (solid lines). Figure 3 shows typical background-subtracted scans obtained using setups 1 and 2.

IV. DATA ANALYSIS AND DISCUSSION

The data were analyzed by least-squares fitting to a parametrized model cross section function that was numerically convoluted with the calculated resolution of the spectrometer. We utilized the same two-Lorentzian representation of the damped harmonic-oscillator cross section for IPA-CuCl₃, as previously employed in the study of finite-temperature effects on gap excitations.²² At each pressure, the parameters of this model are the gap energy Δ , the excitation width (inverse lifetime) Γ , and an overall intensity prefactor:

$$S(\mathbf{q}, \omega) \propto [n(\omega) + 1] \left[\frac{\Gamma}{(\omega - \omega_{\mathbf{q}})^2 + \Gamma^2} - \frac{\Gamma}{(\omega + \omega_{\mathbf{q}})^2 + \Gamma^2} \right], \quad (1)$$

where $n(\omega) + 1$ is the Bose factor and the dispersion relation $\omega_{\mathbf{q}}$ is given by Eq. (2) of Ref. 12.

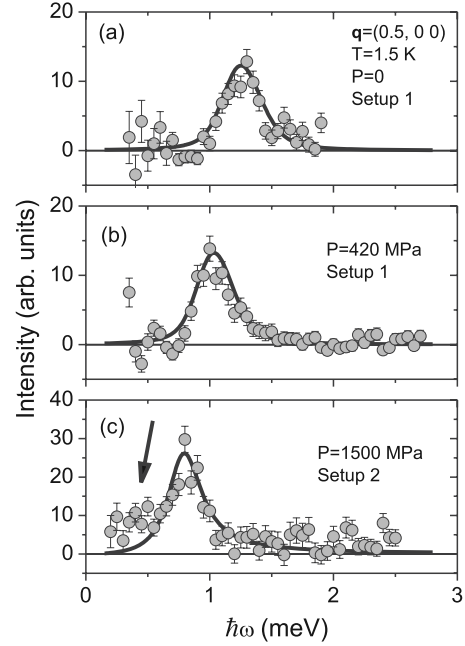


FIG. 3. Background-subtracted constant- q scans collected in IPA-CuCl₃ at the magnetic zone center at various pressures (symbols). The solid lines are fits to the data based on a model cross section function convoluted with the spectrometer resolution, as described in the text. The arrow indicates a broadening of the inelastic peak or extra intensity inside the gap.

For setup 1 good fits to the data are obtained in the entire scan range at all pressures, assuming resolution-limited excitations with $\Gamma \rightarrow 0$. The results are plotted in solid lines in Figs. 3(a) and 3(b). For the 1500 MPa data set measured using setup 2, however, the best fit corresponds to $\Gamma = 0.13(2)$ meV [solid line in Fig. 3(c)]. This intrinsic width primarily accounts for the additional scattering present at low energies [arrow in Fig. 3(c)]. For all experimental pressures the gap energies extracted from the fits are plotted vs pressure in Fig. 4.

In general, it is difficult to carry out inelastic neutron scattering under high pressure because of the limited sample

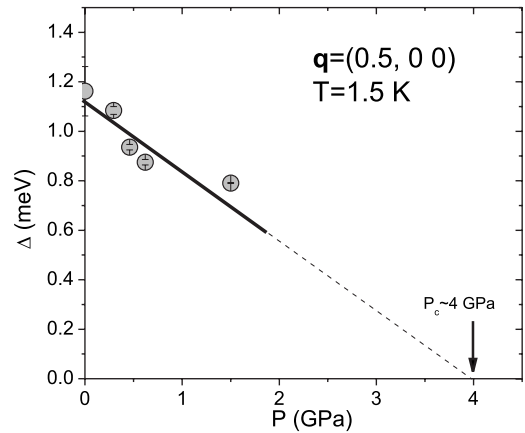


FIG. 4. Pressure dependence of the spin gap in IPA-CuCl₃ measured using inelastic neutron scattering at $T=1.5$ K. A linear extrapolation suggests a soft-mode quantum phase transition at $P_c \approx 4$ GPa.

space and the attenuation of the neutron beam due to the thick walls needed to contain the high pressure. Despite those technical challenges, our neutron results established a steady decrease in the gap energy in IPA-CuCl₃ under applied hydrostatic pressure. The pressure provided by the clamp-type pressure cell is the highest pressure we can reach for the neutron-scattering experiment. While it is not possible to reach the quantum critical point in our experiments, a linear extrapolation of the pressure dependence of Δ suggests that P_c will be close to 4 GPa. Such higher-pressure apparatus is currently unavailable at NCNR. An alternative technique may be high-field magnetization studies that probe the gap indirectly, by detecting the *field-induced* quantum phase transition under applied pressure. In IPA-CuCl₃ the corresponding critical field can be expected to decrease and to reach zero at the pressure-induced critical point.

The pressure dependence of the gap energy in setup 1 with the aluminum He-gas cell at $T=1.5$ K is reversible. The broadening of the inelastic peak at $P=1500$ MPa in setup 2 is to be linked with its drastically increased mosaic spread. It is most likely due to the fractioning of the crystals upon going through the structural phase transition discussed pre-

viously. As established theoretically and experimentally, finite lengths of ladder fragments in a one-dimensional (1D) gapped quantum antiferromagnet will induce a broadening of the gap excitations similar to that at finite temperature.²³ Note that neither the sample mosaic nor the inelastic peaks are affected by pressure in setup 1. The key difference is that in setup 1 the sample was never warmed up above $T \approx 200$ K under pressure, and presumably never went through a phase transition. Any future studies aiming at exploring the incipient quantum phase transition in IPA-CuCl₃ should take heed of this and aim to pressurize the samples at low temperature.

ACKNOWLEDGMENTS

Research at ORNL was funded the Division of Scientific User Facilities, Office of Basic Energy Sciences, U.S. Department of Energy, under Contract No. DE-AC05-00OR22725 with UT-Battelle, LLC. The work at NIST was supported by the National Science Foundation under Agreements No. DMR-9986442, No. DMR-0086210, and No. DMR-0454672.

*Also at Department of Materials Science and Engineering, University of Maryland, College Park, MD 20742, USA.

¹S. Sachdev, *Nat. Phys.* **4**, 173 (2008).

²W. Shiramura, K. Takatsu, H. Tanaka, K. Kamishima, M. Takahashi, H. Mitamura, and T. Goto, *J. Phys. Soc. Jpn.* **66**, 1900 (1997).

³K. Kodama, M. Takigawa, M. Horvatic, C. Berthier, H. Kageyama, Y. Ueda, S. Miyahara, F. Becca, and F. Mila, *Science* **298**, 395 (2002).

⁴C. Rüegg, N. Cavadini, A. Furrer, H.-U. Gudel, K. Kramer, H. Mutka, A. Wildes, K. Habicht, and P. Vorderwisch, *Nature (London)* **423**, 62 (2003).

⁵S. E. Sebastian, P. A. Sharma, M. Jaime, N. Harrison, V. Correa, L. Balicas, N. Kawashima, C. D. Batista, and I. R. Fisher, *Phys. Rev. B* **72**, 100404(R) (2005).

⁶V. O. Garlea, A. Zheludev, T. Masuda, H. Manaka, L.-P. Regnault, E. Ressouche, B. Grenier, J.-H. Chung, Y. Qiu, K. Habicht, K. Kiefer, and M. Boehm, *Phys. Rev. Lett.* **98**, 167202 (2007).

⁷T. Giamarchi, C. Rüegg, and O. Tchernyshev, *Nat. Phys.* **4**, 198 (2008).

⁸D. Schmeltzer and A. R. Bishop, *Phys. Rev. B* **58**, R5905 (1998).

⁹H. Tanaka, K. Goto, M. Fujisawa, T. Ono, and Y. Uwatoko, *Physica B* **329-333**, 697 (2003).

¹⁰C. Rüegg, A. Furrer, D. Sheptyakov, T. Strassle, K. W. Krämer, H.-U. Gudel, and L. Mélési, *Phys. Rev. Lett.* **93**, 257201 (2004).

¹¹C. Rüegg, B. Normand, M. Matsumoto, A. Furrer, D. F. McMorrow, K. W. Kramer, H.-U. Gudel, S. N. Gvasaliya, H. Mutka,

and M. Boehm, *Phys. Rev. Lett.* **100**, 205701 (2008).

¹²T. Masuda, A. Zheludev, H. Manaka, L.-P. Regnault, J.-H. Chung, and Y. Qiu, *Phys. Rev. Lett.* **96**, 047210 (2006).

¹³H. Manaka, I. Yamada, and K. Yamaguchi, *J. Phys. Soc. Jpn.* **66**, 564 (1997).

¹⁴H. Manaka, I. Yamada, Z. Honda, H. A. Katori, and K. Katsumata, *J. Phys. Soc. Jpn.* **67**, 3913 (1998).

¹⁵A. Zheludev, V. O. Garlea, T. Masuda, H. Manaka, L.-P. Regnault, E. Ressouche, B. Grenier, J.-H. Chung, Y. Qiu, K. Habicht, K. Kiefer, and M. Boehm, *Phys. Rev. B* **76**, 054450 (2007).

¹⁶K. Koyama, T. Goto, T. Kanomata, and R. Note, *J. Phys. Soc. Jpn.* **68**, 1693 (1999).

¹⁷S. A. Roberts, D. R. Bloomquist, R. D. Willett, and H. W. Dodgen, *J. Am. Chem. Soc.* **103**, 2603 (1981).

¹⁸G. E. Granroth, S. Maegawa, M. W. Meisel, J. Krzystek, L.-C. Brunel, N. S. Bell, J. H. Adair, B. H. Ward, G. E. Fanucci, L.-K. Chou, and D. R. Talham, *Phys. Rev. B* **58**, 9312 (1998).

¹⁹H. Manaka and I. Yamada, *J. Phys. Soc. Jpn.* **66**, 1908 (1997).

²⁰A. Onodera, Y. Nakai, N. Kunitomi, O. A. Pringle, H. G. Smith, R. M. Nicklow, R. M. Moon, F. Amita, N. Yamamoto, S. Kawano, N. Achiwa, and Y. Endoh, *Jpn. J. Appl. Phys., Part 1* **26**, 152 (1987).

²¹I. A. Zaliznyak, D. C. Dender, C. Broholm, and D. H. Reich, *Phys. Rev. B* **57**, 5200 (1998).

²²A. Zheludev, V. O. Garlea, L.-P. Regnault, H. Manaka, A. Tsvelik, and J.-H. Chung, *Phys. Rev. Lett.* **100**, 157204 (2008).

²³G. Xu, C. Broholm, Y.-A. Soh, G. Aeppli, J. F. DiTusa, Y. Chen, M. Kenzelmann, C. D. Frost, T. Ito, K. Oka, and H. Takagi, *Science* **317**, 1049 (2007).